Supplementary Information:
Regulation of minimal spindle midzone organization by mitotic kinases

Wei Ming Lim[1], Wei-Xiang Chew[1], Arianna Esposito Verza[2], Marion Pesenti[2], Andrea Musacchio[2,3,4], Thomas Surrey[1,5,6]

[1] Centre for Genomic Regulation (CRG), The Barcelona Institute of Science and Technology, Carrer del Dr. Aiguader 88, Barcelona 08003, Spain
[2] Department of Mechanistic Cell Biology, Max Planck Institute of Molecular Physiology, Dortmund, Germany
[3] Max Planck School Matter to Life, Heidelberg, Germany
[4] Centre for Medical Biotechnology, Faculty of Biology, University Duisburg-Essen, Essen, Germany
[5] Universitat Pompeu Fabra (UPF), Barcelona, Spain
[6] Catalan Institution for Research and Advanced Studies (ICREA), Passeig de Lluis Companys 23, Barcelona 08010, Spain

The file includes:

8 Supplementary Figures and Legends
7 Supplementary Movie Legends

Supplementary Figure 1

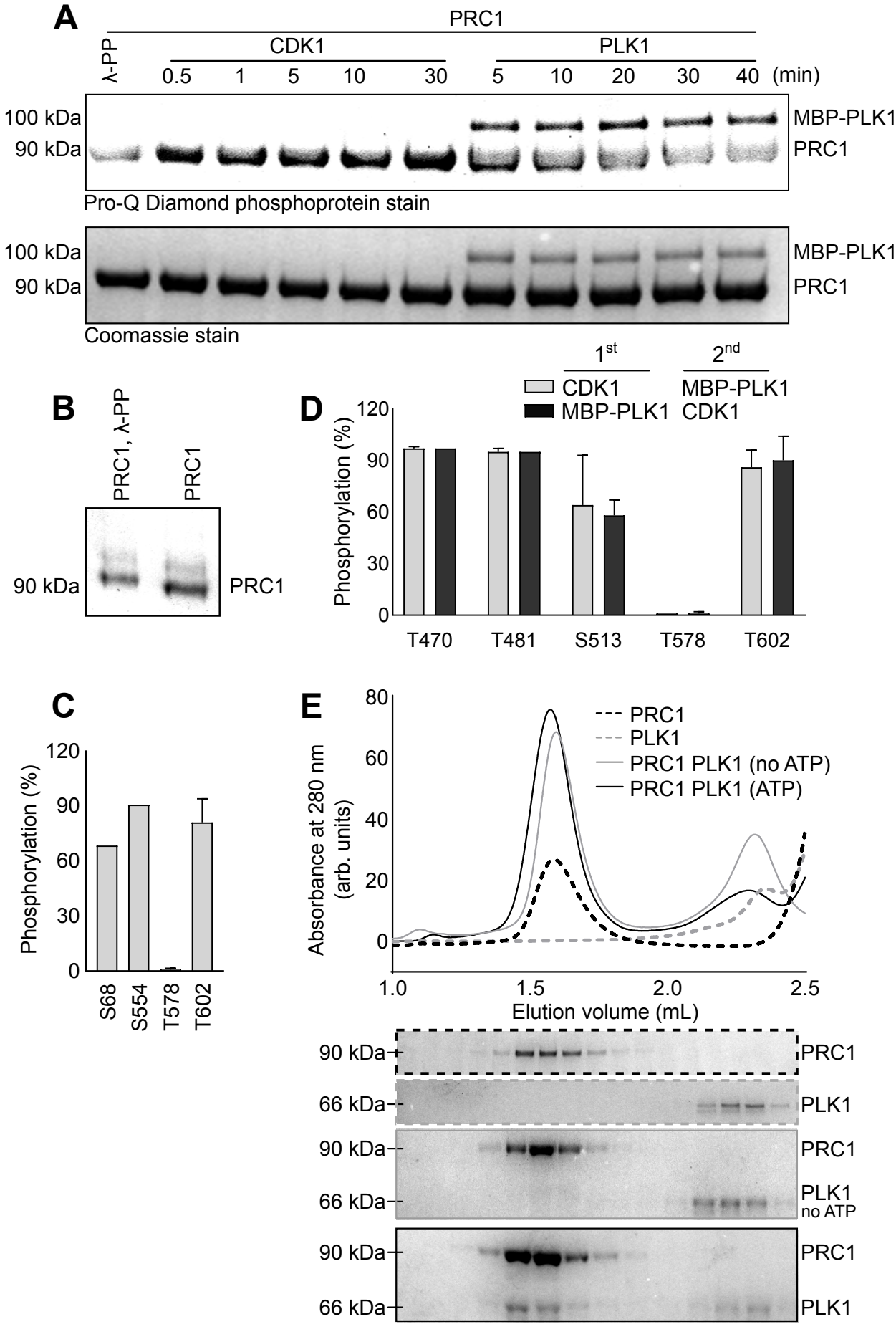

Supplementary Figure 1. Phosphorylation of PRC1 by CDK1 and PLK1 and polo-box binding. (A) Pro-Q Diamond phosphoprotein (top) and Coomassie (bottom) stain of samples as shown in Fig. 1A. **(B)** Phos-tag gel of 5 µM PRC1-SNAP incubated with and without lambda protein phosphatase (λ-PP) for 30 min, showing that purified PRC1 is essentially unphosphorylated. (**C**) Mass-spectroscopic quantification of the degree of phosphorylation of PRC1 residues serine 68, 554 and threonine 578, 602 (S68, S554, T578, T602) by 1 µM MBP-PLK1 for 30 min. Data are presented as mean and errors bars are standard deviation. n = 5 independent experiments for residues T578 and T602, and n = 1 experiment for residue S68 and S554. (**D**) Mass spectroscopic quantification of the degree of phosphorylation of PRC1 residues after phosphorylating PRC1 first with 170 nM CDK1/Cyclin B/CKS1 for 5 min, then with 1 µM MBP-PLK1 for 30 min (grey) or after phosphorylating PRC1 first with 1 µM MBP-PLK1 for 30 min, then with 170 nM CDK1/Cyclin B/CKS1 for 5 min (black) at 4 °C. All PRC1 residues of interest showed essentially the same degree of phosphorylation independent of the order of phosphorylation, indicating that the kinases do not promote or inhibit each other's phosphorylation. Data are presented as mean and the error bars are standard deviation. n = 2. (**E**) UV absorbance profile (top) and corresponding Coomassie-stained SDS gel fractions (bottom) of size exclusion chromatography runs of 5 µM PRC1 or 5 µM His-PLK1 or both mixed together either in the presence or absence of ATP, as indicated, and incubated for 30 min at 4 °C. The shift of the absorbance profile and of the elution volumes of PRC1 and a major fraction of PLK1 to a smaller volume in the experiment with both proteins being mixed in the presence of ATP indicates binding of PLK1 to PLK1-phosphorylated PRC1.

Supplementary Figure 2

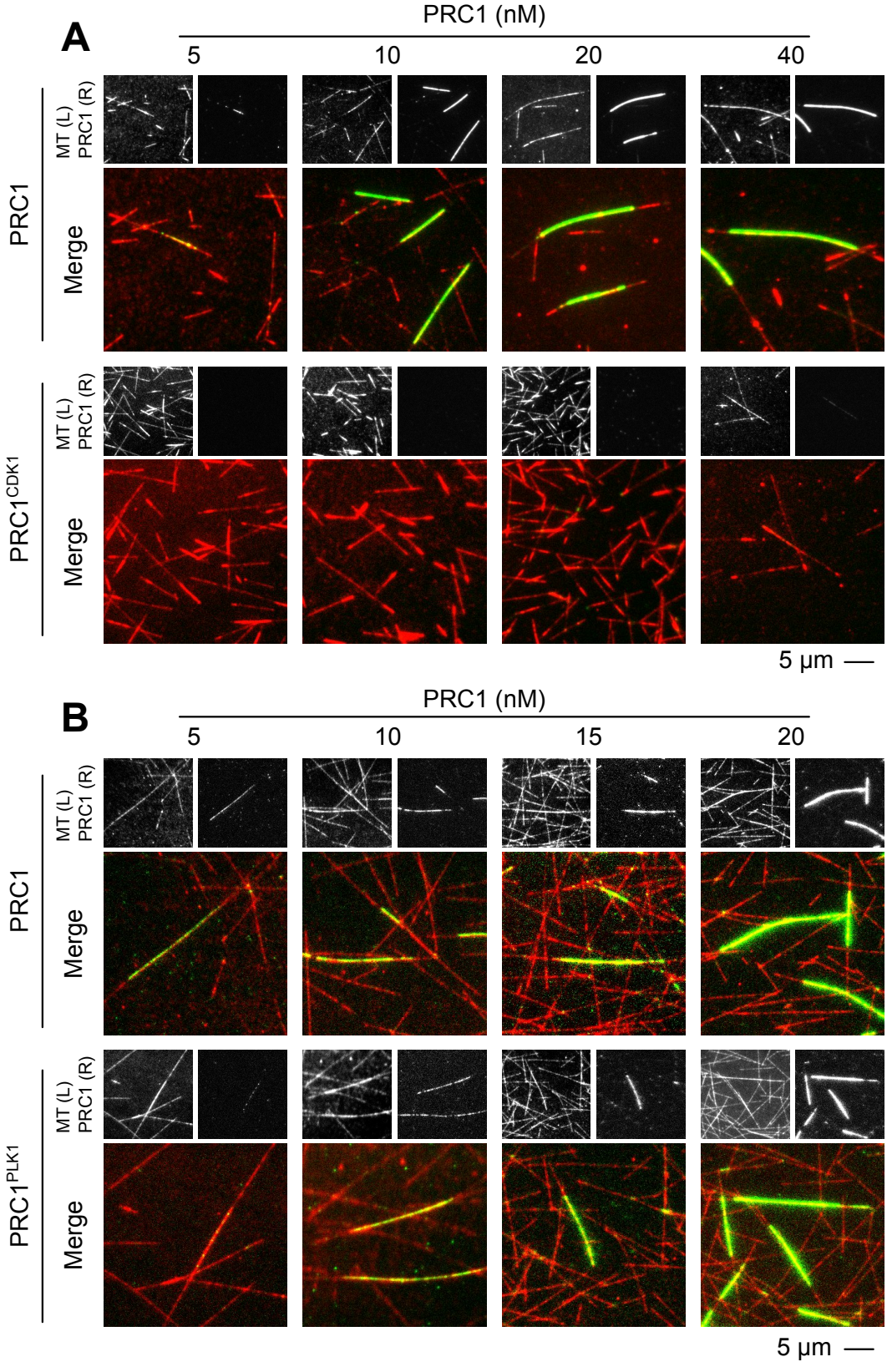

Supplementary Figure 2. Unphosphorylated, CDK1-phosphorylated and PLK1-phosphorylated PRC1 binding to antiparallel microtubule overlaps. Same data as shown **(A)** in Fig. 2B and **(B)** in Fig. 2D, but now displaying in addition to the merged PRC1-Alexa546 (green) and Alexa647-microtubule (red) images also the microtubule (top left) and PRC1 (top right) images separately in greyscale. Segments with high PRC1 intensity correspond to antiparallel microtubule overlaps. PRC1 concentrations and scale bars as indicated.

Supplementary Figure 3

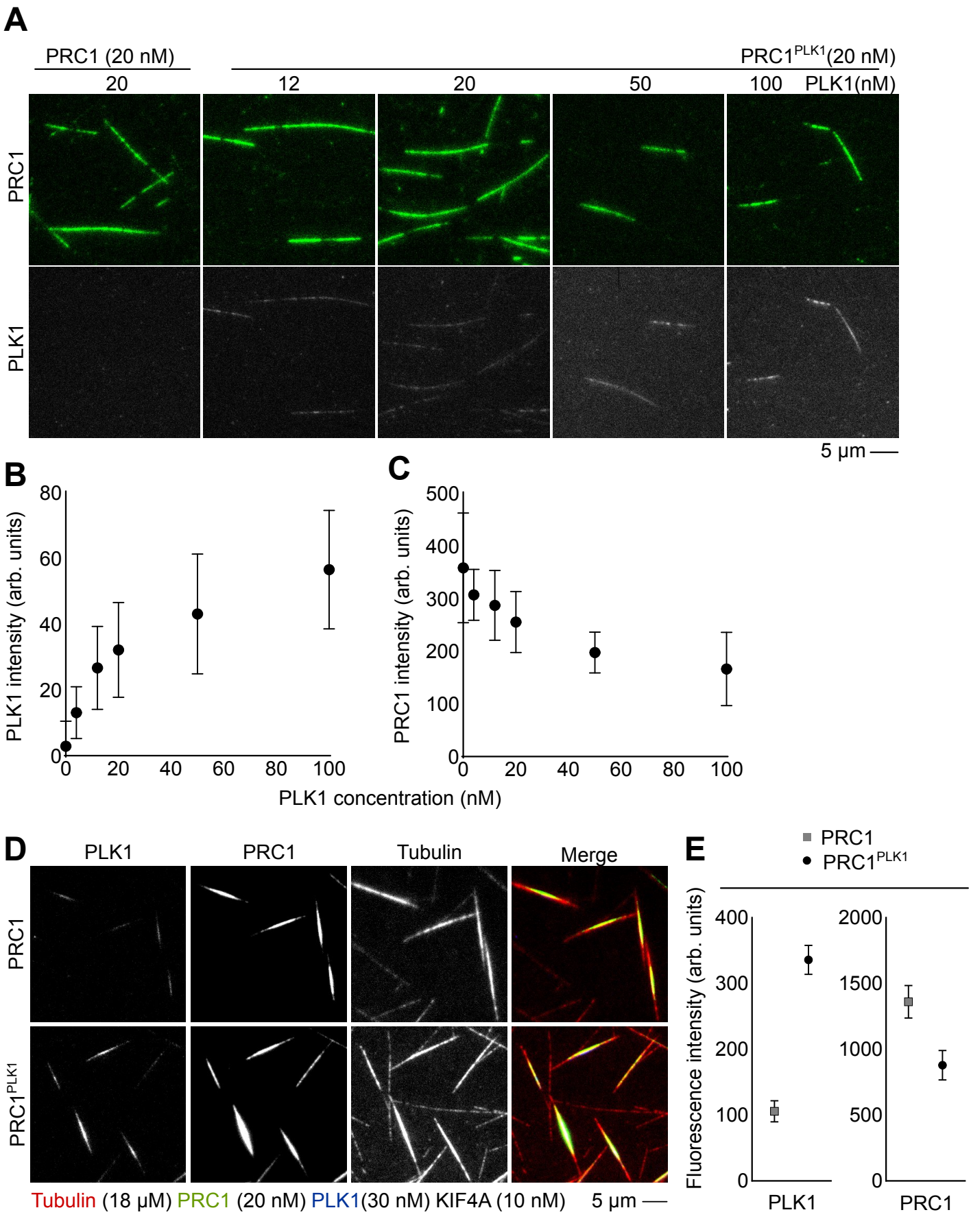

Supplementary Figure 3. Phosphorylation of PRC1 by PLK1 leads to PLK1 recruitment to antiparallel microtubule overlaps. (A) TIRF microscopy images of 20 nM fluorescein-PLK1-pre-phosphorylated PRC1-Alexa546 binding to antiparallel microtubule overlaps (top), recruiting increasing amounts of fluorescein-PLK1 to the overlaps (same assay as in Fig. 2D). Fluorescein-PLK1 concentrations and scale bar as indicated. **(B)** Quantified mean fluorescein-PLK1 intensity and **(C)** quantified mean PRC1-Alexa546 intensity in antiparallel microtubule overlaps. Error bars are standard deviation. $n = 3$, total length of 100 μm of antiparallel overlaps for each tested concentration. The reduction of PRC1 intensity with increasing PLK1 concentration likely indicates a certain degree of steric hindrance between the two proteins in the microtubule overlap region. **(D)** TIRF microscopy images taken ~10 minutes after self-organization of microtubule bundles in the presence of 20 nM unphosphorylated-PRC1 (top) and fluorescein-PLK1-phosphorylated (bottom) PRC1-Alexa546 (green), 10 nM KIF4A (unlabelled), 18 μM Alexa647-tubulin (red) and 30 nM fluorescein-PLK1 (blue). Scale bar as indicated. **(E)** Quantification of mean fluorescein-PLK1 and mean PRC1-Alexa546 fluorescence intensity measured in antiparallel overlap microtubule bundles for unphosphorylated and fully PLK1-phosphorylated PRC1. The mean fluorescence intensity for Alexa647-tubulin is 1927.9 ± 123.4 and 1967.4 ± 171.2 (a.u.) respectively. Error bars are standard error. $n = 2$, 30 antiparallel bundles.

Supplementary Figure 4

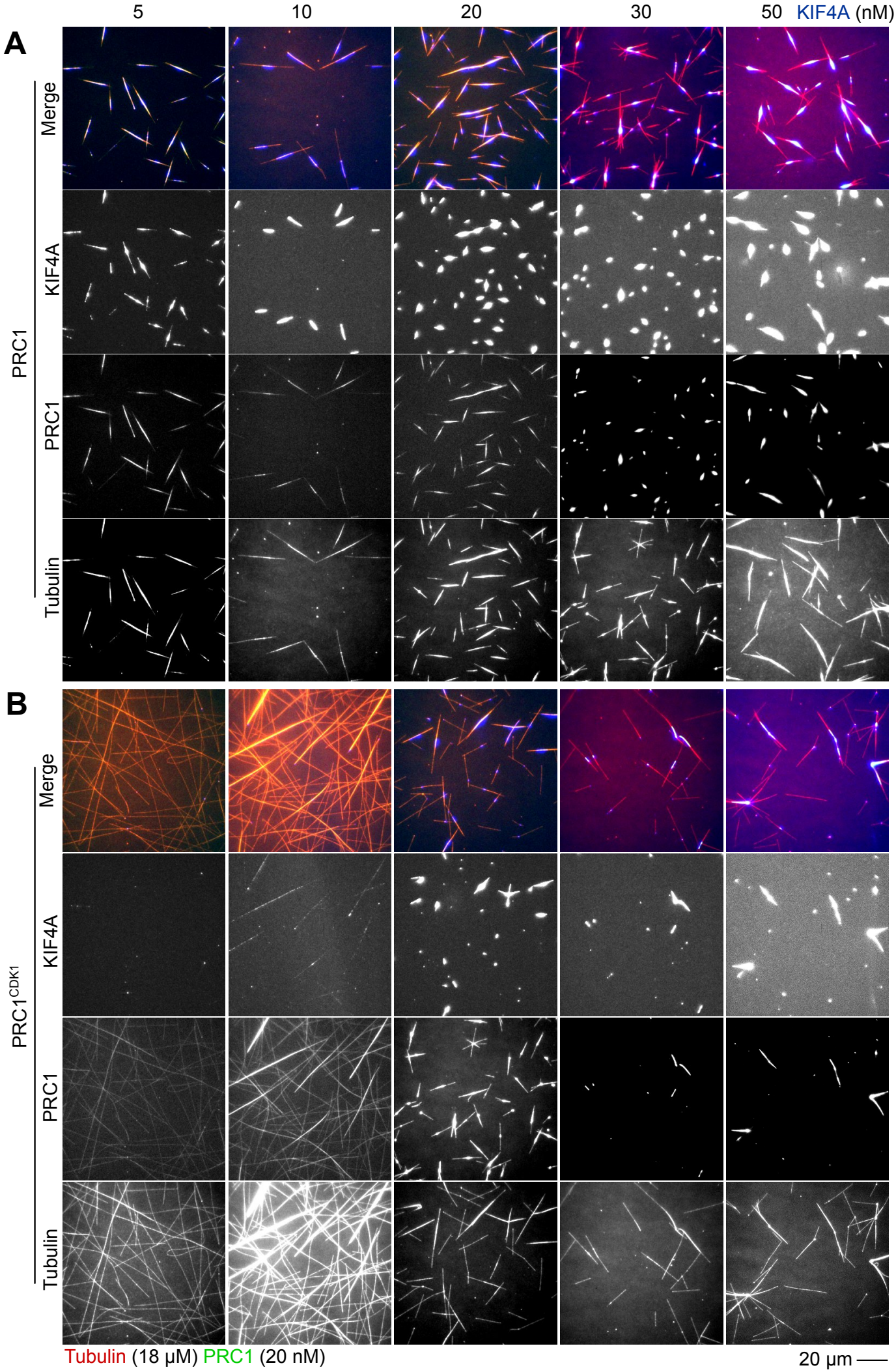

Supplementary Figure 4. Together with KIF4A, unphosphorylated and CDK1-phosphorylated PRC1 organize different microtubule bundle architectures. Same data as shown **(A)** in Fig. 3B (top) and **(B)** in Fig. 3B (bottom), but now displaying in addition to merged images, also individual images of Alexa647-microtubules, PRC1-Alexa546 and KIF4A-mGFP in greyscale.

Supplementary Figure 5

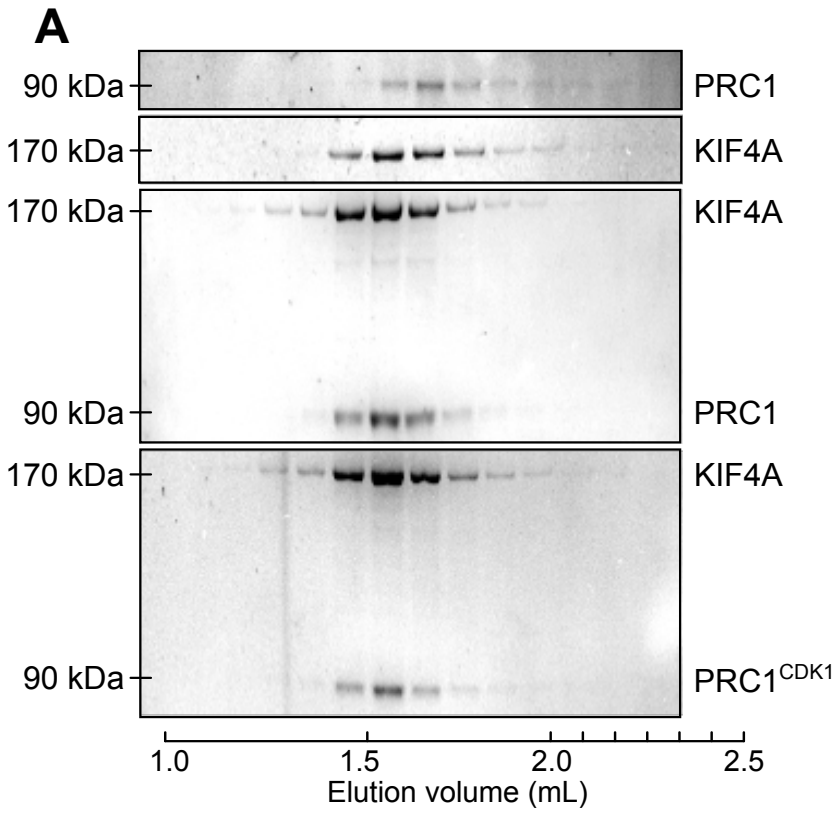

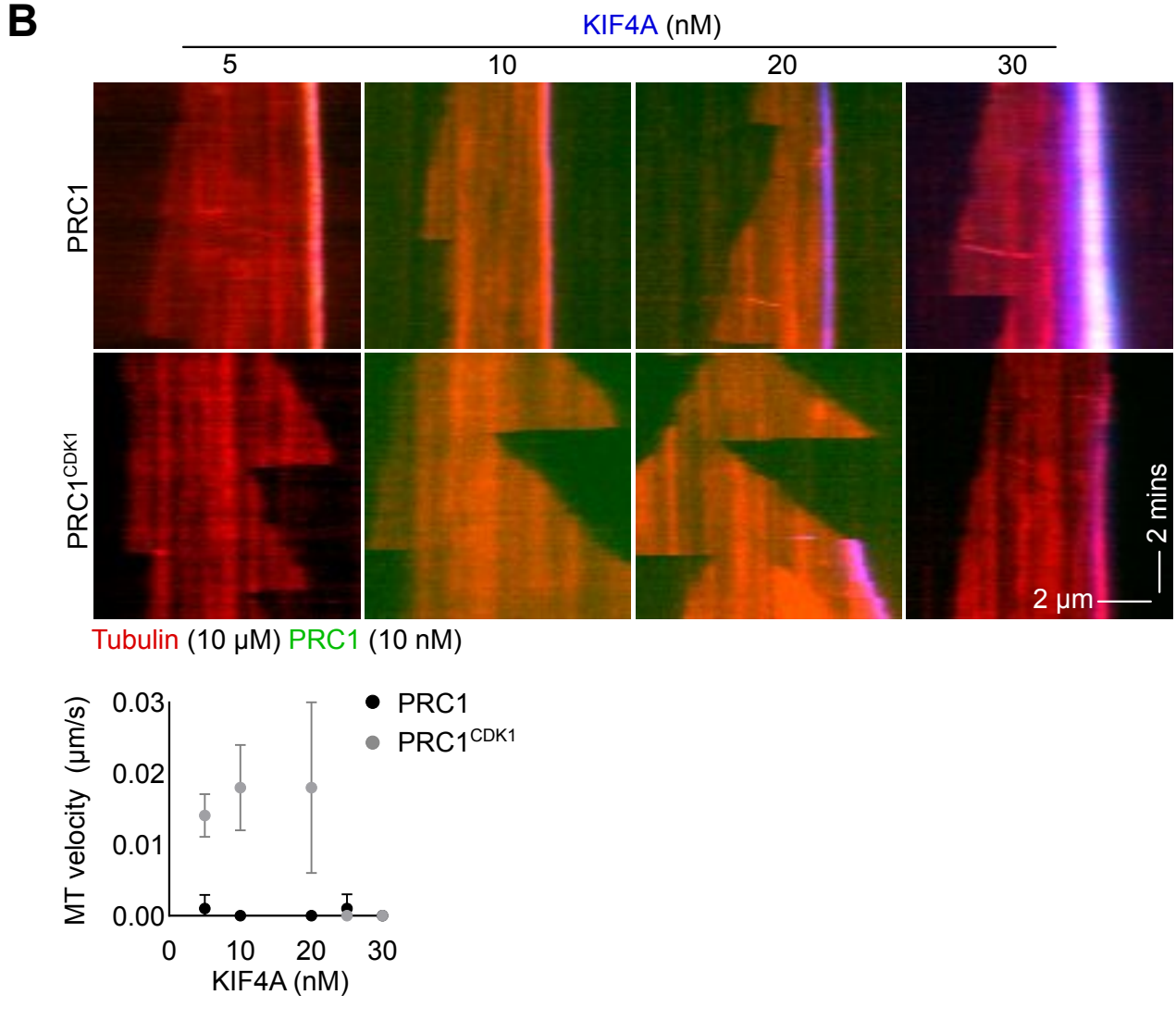

Supplementary Figure 5. Phosphorylation of PRC1 by CDK1 indirectly controls KIF4A recruitment to microtubules. (A) Analytical size exclusion chromatography: Coomassie-stained SDS gels of unphosphorylated PRC1-SNAP, KIF4A-mGFP or mixtures of unphosphorylated or CDK1-phosphorylated PRC1-SNAP together with KIF4A eluted from a gel filtration column at the indicated volumes**.** Concentrations were 5 μM PRC1 and 5 μM KIF4A-mGFP. When mixed PRC1 and KIF4A co-migrate independently of the phosphorylation state of PRC1, indicating that their interaction is unaffected by the phosphorylation of PRC1. **(B)** TIRF microscopy kymographs of individual microtubules growing from surface-immobilized stabilized microtubule seeds in the presence of 10 μM Alexa647-tubulin (red), 10 nM unphosphorylated (top) or CDK1-phosphorylated (bottom) PRC1-Alexa547 (green) and 5 - 30 nM KIF4A (blue). Scale bars as indicated. The plot shows quantified mean microtubule growth velocities in the presence of unphosphorylated (black) and CDK1-phosphorylated PRC1 (grey) at different KIF4A concentrations. Error bars are standard deviation. $n = 3$. Whereas at all tested KIF4A concentrations, plus-end growth was stopped in the presence of non-phosphorylated PRC1, plus ends still grew in the presence of the three lower KIF4A concentrations in the presence of phosphorylated PRC1, indicating that less KIF4A is recruited to the microtubules when less PRC1 binds due to its lower affinity caused by phosphorylation by CDK1.

Supplementary Figure 6

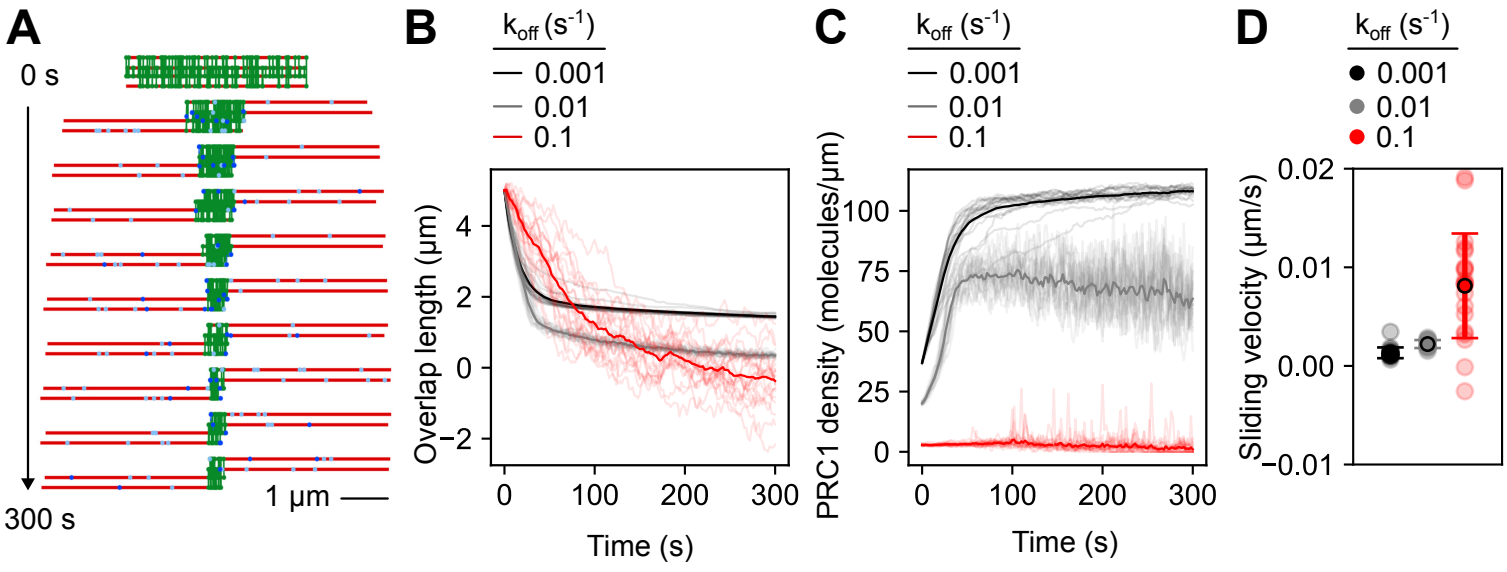

Supplementary Figure 6. Computer simulations of minimal midzone formation. (A) Exemplary snap shots of the temporal development of a simulated bundle consisting of 4 microtubules (red) connected by PRC1 (green) and KIF4A (blue). **(B)** Average antiparallel overlap length of 10 simulated microtubule bundles per condition as a function of time. The PRC1 unbinding rate (k_{off}) from microtubules differed between conditions, as indicated. Increasing the unbinding rate reduces PRC1 affinity to microtubules, which reproduces the effect of PRC1 phosphorylation in the experiment. **(C)** Average linear PRC1 density over time and **(D)** the individual and mean antiparallel microtubule sliding velocities (calculated from time 100 s to 300 s) of the same simulated bundles. Erros bars are standard deviation. Thick and thin lines represent the mean and individual overlap lengths and PRC1 densities, respectively.

Supplementary Figure 7

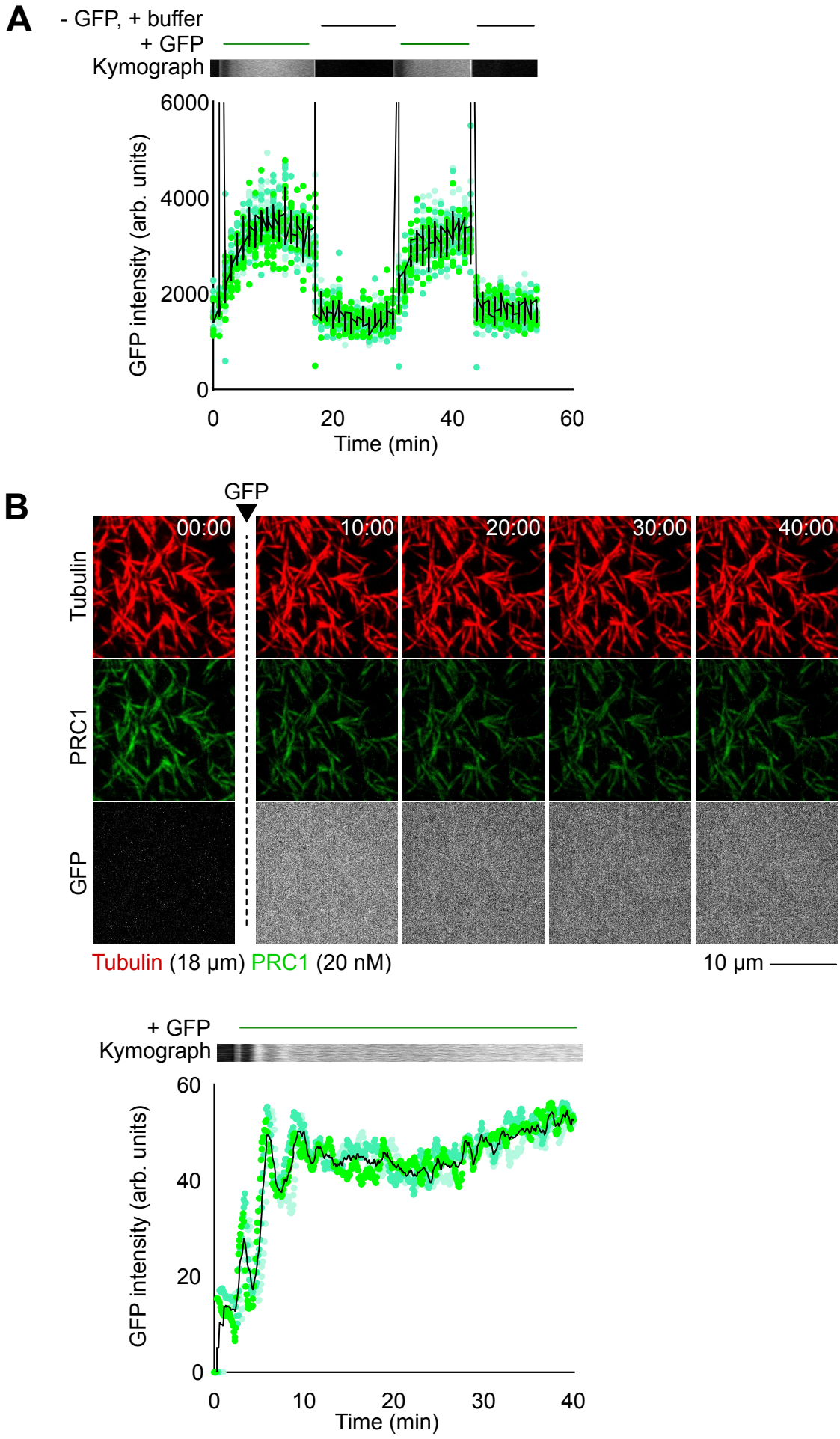

Supplementary Figure 7. Characterization of diffusive protein delivery to the microscopy chamber from the top reservoir. (A) Time course of fluorescence intensity measured in the observation chamber by TIRF microscopy, while the buffer in the top reservoir was repeatedly exchanged either containing 400 nM GFP or not. **(B)** Confocal fluorescence microscopy images of Alexa647-microtubule bundles (red) formed in a solution containing 20 nM PRC1-Alexa546 (green) and 18 μM Alexa647-tubulin, imaged before and after the addition of 400 nM GFP (grey) to the top reservoir for delivery to the observation chamber by diffusion. Times in min:sec, scale bar as indicated. The experiment shows that diffusive protein delivery does not induce turbulence, because the bundles (which are not surface-attached) do not move after GFP delivery.

Supplementary Figure 8

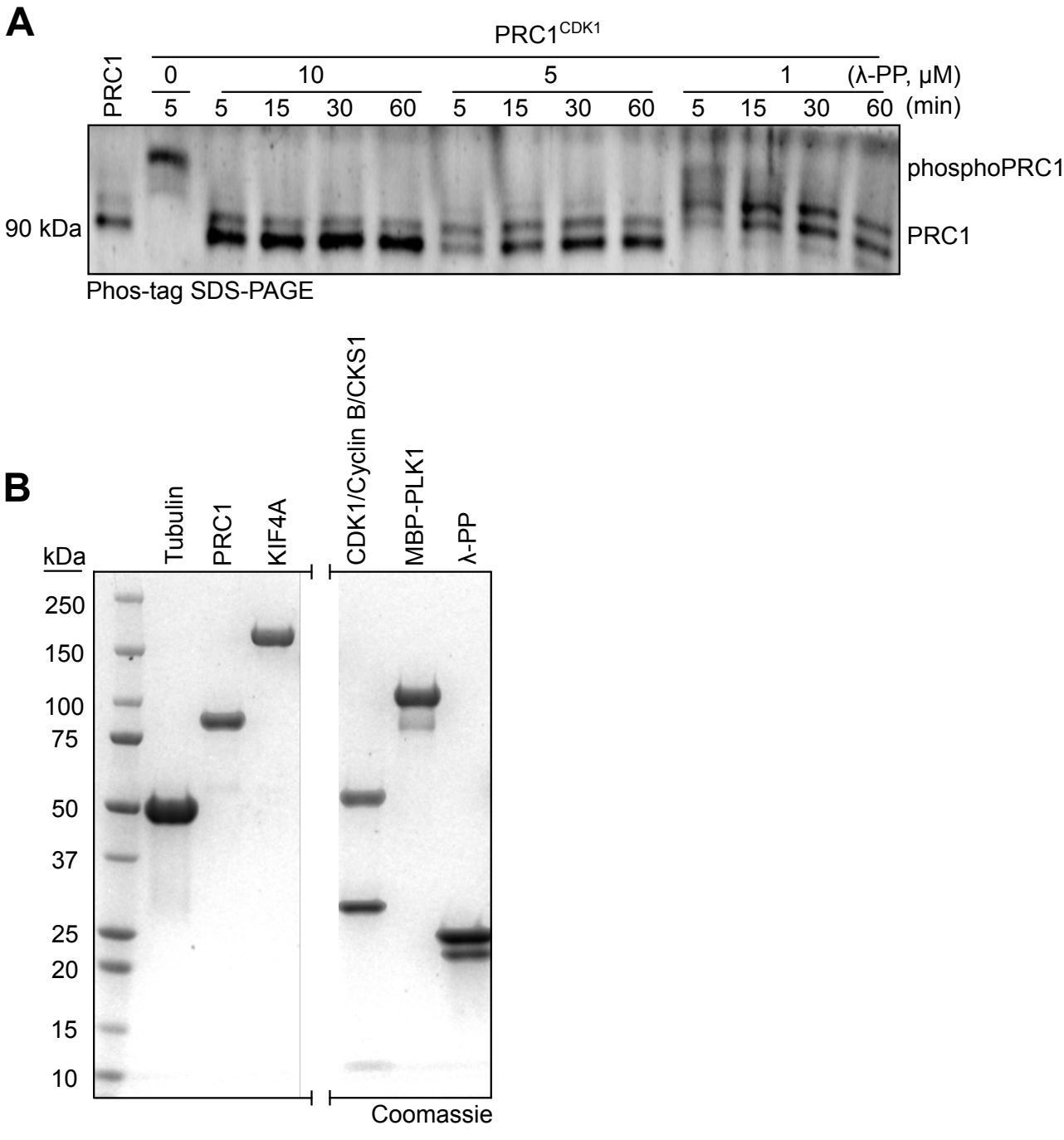

Supplementary Figure 8. (A) Dephosphorylation of CDK1-phosphorylated PRC1 by lambda phosphatase: SYPRO-Ruby stained Phos-tag gel of 800 nM CDK1-phosphorylated PRC1-SNAP incubated with 10, 5 or 1 μM lambda protein phosphatase (λ-PP) for the indicated times, or unphosphorylated and CDK1-phosphorylated PRC1-SNAP as negative and positive control. **(B) Coomassie-stained SDS gel of purified proteins:** porcine brain tubulin, and recombinant PRC1, KIF4A, CDK1/cyclin b/CKS1, MBP-PLK1 and λ-PP used in this study.